

A new metal–organic hybrid material with intrinsic resistance-based bistability: monitoring *in situ* room temperature switching behavior†

Cite this: *J. Mater. Chem. C*, 2014, 2, 399

Zhongyue Zhang,^{ab} Hanhua Zhao,^a Michio M. Matsushita,^b Kunio Awaga^b and Kim R. Dunbar^{*a}

Received 12th August 2013
Accepted 11th November 2013

DOI: 10.1039/c3tc31577k

www.rsc.org/MaterialsC

Two new silver containing materials with TCNQ derivatives were prepared by electrocrystallization. Synchrotron radiation diffraction studies were conducted to determine the structures of the new phases which exhibit unprecedented high room temperature conductivity. The *I*–*V* characteristics reveal a room-temperature switching behaviour and memory effect based on intrinsic negative differential resistance (NDR). EPR spectroscopic measurements performed under an applied electric field indicate a *g*-tensor shift that is correlated to the amplitude of current.

Resistance-based bistability in materials is highly relevant to the future development of electronic devices in which a high resistance “OFF” state rapidly switches to a low resistance “ON” state as a result of external stimulation. The use of different stimuli to trigger the switching process has unearthed a variety of phenomena including magnetoresistivity (response to an external magnetic field),¹ piezoresistivity (response to mechanical pressure),² photoresistivity (response to light),³ and direct non-linear resistance (response to the strength of electric field).⁴ Given that the timescale of switching is very fast, materials in these categories are being sought for incorporation into new types of electronic devices. The interest in these materials stems from the fact that they are not just merely stimuli-responsive sensors; their properties reflect an interplay between the external field and the electric response which has promise in fast data processing for random access memory applications (RAM). The memory effect arises from the “ON” and “OFF” states which are able to represent “0” and “1” in data processing and storage. RAMs are differentiated into two categories based on whether the data can be maintained after the external stimulus is removed. Dynamic RAM (DRAM) refers to volatile memory that loses its memory effect when the power supply is removed, but its fast write–erase speed and high circular write–erase numbers makes it ideal for temporary storage (main memory) for the central processing unit (CPU). Non-volatile RAM (NVRAM)

maintains the memory effect without the power supply which translates to permanent information storage. Advances in technologies involving computation and data storage continue to rely heavily on the development of DRAM and NVRAM.⁵

Given the requirement of reduction in device size and enhancement of processing speeds for vastly improved information technology, there is an intense effort to realize ever-increasing memory storage density and fast processing speeds.⁶ Most traditional RAM devices are based on solid-state semiconductors such as silicon chips⁷ and metal oxides,^{8,9} whose size limits are determined by the limitations of fabrication. In this regard, molecule-based bistable materials are attracting considerable attention in recent years because they can respond to the aforementioned stimuli but have much smaller domain sizes on the order of a molecule. Recent advances in the field of molecular materials include the discovery of simple organic compounds that exhibit intrinsic bistability such as ferroelectrics that can be used as non-volatile memory with long retention times.¹⁰ Two elegant examples of very simple organic compounds that exhibit extraordinary properties have recently reported, namely donor–acceptor (D–A) charge transfer salts based on pyromellitic diimide-based acceptors¹¹ and diisopropylammonium bromide.¹² Phase transition induced temperature-dependent spontaneous polarization is observed in these materials which can be controlled by an external electric field or mechanical forces. The remarkable performance of these simple organic-based materials meet the stringent requirements of a successful device, *viz.*, ease of preparation, stability and room-temperature performance and, importantly purity that insures that the property is intrinsic to the material which guarantees high performance. In fact, such organic materials are candidates for modern ferroelectric RAM (FeRAM) which is a promising alternative to traditional flash memory.¹³

^aDepartment of Chemistry, Texas A&M University, P.O. Box 30012, College Station, TX, 77842, USA. E-mail: dunbar@mail.chem.tamu.edu; Fax: +1-979-845-7177; Tel: +1-979-845-5235

^bDepartment of Chemistry, Nagoya University, Furo-cho, Chikusa, Nagoya, 464-8601, Japan

† Electronic supplementary information (ESI) available. CCDC 924677 and 924678. For ESI and crystallographic data in CIF or other electronic format see DOI: 10.1039/c3tc31577k

Apart from purely organic materials, another important category of compounds *vis-à-vis* resistive switching behaviour is metal–organic hybrid materials. To date, the most extensively studied examples are the binary phases Cu(TCNQ) and Ag(TCNQ) (TCNQ = 7,7,8,8-tetracyanoquinodimethane), a family of compounds formed by spontaneous redox reactions of the group 11 metal with neutral TCNQ molecules. It was discovered in 1979 that thin films of these materials exhibit a remarkable transition in their electrical properties with the application of an electric field or upon irradiation.^{14,15} In the case of Cu(TCNQ) a sandwich device composed of Cu/Cu(TCNQ)/Al was prepared by growing the film on a Cu electrode by spontaneous electrolysis which exhibits a sharp resistance state change from nearly insulating (2 MΩ) to a low resistance state (200 Ω) at a field strength of $4 \times 10^3 \text{ V cm}^{-1}$; full recovery to the high resistance state was observed upon application of an electric field in the opposite direction. The devices based on these materials are highly compatible for the application of new generation NVRAM due to the fast switching behaviour and the convenience and low cost preparation by a self-assembly process. The discovery of the remarkable properties exhibited by these materials spawned a large number of studies directed at the fabrication of device-friendly structures including nanowires, nanoribbons and nanosize fabricated micro-devices.^{16–21}

Throughout the decades of research on Cu(TCNQ) and related materials, a great deal of attention has been directed at understanding the mechanism of the non-linear response of the external voltage and switching properties of M(TCNQ) materials. Techniques that proved to be useful at providing details include *in situ* Raman spectroscopy, X-ray photoelectron spectroscopy (XPS) and ultrafast electron microscopy, the collective results of which point to the fact that the material undergoes partial decomposition and that the presence of metal atoms/islands are responsible for the switching behavior (Scheme 1).^{22–26} In the case of Cu(TCNQ), the transition from the “OFF” state to the “ON” state has been postulated to result in the production of Cu(0) and TCNQ⁰ as a result of an electric field induced ligand-to-metal electron transfer (LMCT). The presence of Cu metal in the material, would then, drastically enhance the conductivity and lead to a low resistance state. Although the presence of Cu⁰ and TCNQ⁰ has been detected by different methods, the actual mechanism has not yet been definitively ascertained because real time observation under electric field has never been reported.

One of the issues with the switching behavior of the originally prepared Cu(TCNQ) material over the years has been unrecognized polymorphism which is now known to exert a profound effect on the reproducibility of the devices. The Cu/Cu(TCNQ) film/Al sandwich devices have been found to exhibit a sharp switching response under an applied voltage,

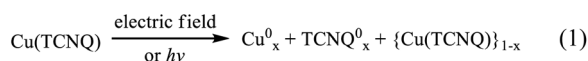
but the resistivity behaviour depends on the exact conditions of film preparation because of the presence of more than one polymorph.^{15,18,27–32} The difficulty of separating and characterizing pure crystalline phases of these distinct polymorphs is a major obstacle for understanding their physical properties. It was not until 1999, however, when we successfully obtained the first samples of very small single crystals of Cu(TCNQ) that it was finally realized that there are two distinct polymorphs with completely different resistivity behavior.³³ The highly conducting polymorph (phase I) adopts a perpendicular arrangement of adjacent TCNQ columns and is responsible for the switching behaviour in the device, whereas phase II is nearly insulating at room temperature.

Another main subject of scrutiny *vis-à-vis* this type of switching behaviour is the related material Ag(TCNQ) whose structure was first reported by Shields.³⁴ The material is also suspected to be polymorphic based on infrared spectral and powder XRD patterns but this has not been verified by single crystal X-ray data.^{35,36} Clearly, structural characterization of these molecule-based materials is critical for a deep understanding of the physical behaviour but it is notoriously difficult to obtain single crystals.

In contrast to the plethora of studies conducted over the years on the TCNQ-based materials, corresponding derivatives of TCNQ are essentially unknown in terms of their solid-state properties. Many substituted derivatives of TCNQ are known,³⁷ with tunable electronic and steric properties, but their tedious preparation, low yields, thermal decomposition and air sensitivity has hampered extensive research on these acceptors. In recent years, our group has been focusing on 2,5-dihalogen substituted TCNQ derivatives, namely TCNQX₂ (X = Cl, Br).⁴¹ By incorporating the radical form of these ligands into network solids with the Cu(I) cation, two unprecedented semi-conducting materials Cu(TCNQCl₂) and Cu(TCNQBr₂) were prepared in 2010³⁸ and were found to exhibit enhanced conductivity. As compared to the original Cu(TCNQ) material, the room temperature conductivities are 1.15 and 0.27 S cm^{−1}, respectively, with the former value being the highest among the family of 1 : 1 M⁺ : TCNQ[−] salts.

Herein we report two crystalline materials Ag(TCNQCl₂), (1), and Ag(TCNQBr₂), (2) synthesized by electrocrystallization using a silver electrode in contact with an acetonitrile solution of TCNQX₂, a method that was originally used in 1985 to grow Ag(TCNQ) crystals.³⁴ Compound 1 exhibits a room temperature conductivity of 0.25 S cm^{−1} and a current-induced switching behaviour at room temperature whereas compound 2 is nearly insulating.

Crystals of the new compounds are very small and suffer from twinning problems therefore synchrotron radiation diffraction experiments were performed at 110 K.⁴² The structure of 1 (Fig. 1) is a three-dimensional network with Ag(I) ions coordinated to four adjacent TCNQCl₂[−] radicals in a highly distorted tetrahedral environment with N–Ag–N angles of 97.75°, 103.77°, 126.53° and 131.04°. The columns of stacked TCNQCl₂[−] radicals are oriented along the *b* axis with a homogenous separation of 3.23 Å which is similar to the



Scheme 1 The proposed mechanism for Cu(TCNQ) switching. Ag(TCNQ) is thought to adopt a similar mechanism.

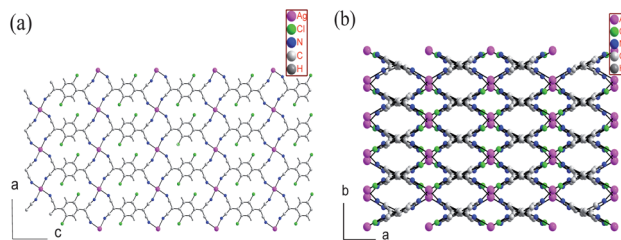


Fig. 1 Structure of $\text{Ag}(\text{TCNQCl}_2)$, (1): (a) viewed in the ac plane and (b) in the ab plane.

distance of 3.24 Å found in the $\text{Cu}(\text{TCNQ})$ phase I;³³ adjacent columns exhibit a dihedral angle of 135.3° .

The structure of compound 2 (Fig. 2) is also that of a 3D network and is best described as a stack of slightly distorted 2-D layers in which $\text{Ag}(\text{i})$ cations in an unprecedented arrangement with six TCNQBr_2^- radicals engaged in four in-plane $\text{Ag}-\text{N}$ bonds of 2.197, 2.226, 2.572 and 3.082 Å and two inter-layer $\text{Ag}-\text{N}$ bonds of 2.616 and 2.675 Å. The adjacent columns of TCNQBr_2^- radicals, which are oriented in a parallel manner, do not overlap perfectly along the a axis. The alternating separation distance of TCNQ radicals along the column (3.23 and 3.03 Å) indicates a high degree of dimerization of radicals in the stacks. In both 1 and 2, the separation distances between adjacent TCNQ molecules are much shorter than the sum of van der Waals radii of the halogen atoms (3.60 Å for $\text{Cl}-\text{Cl}$ and 3.80 Å for $\text{Br}-\text{Br}$), which further supports the fact that there are strong interactions between the neighboring radicals in the stacks.

Infrared spectral data are highly useful for diagnosing the charge and coordination strength of the TCNQ radicals. For both 1 and 2, two strong ν_{CN} modes are observed (2189 cm^{-1} and 2165 cm^{-1} for 1, 2187 cm^{-1} and 2160 cm^{-1} for 2) which are indicative of coordinated TCNQ radicals. For comparison sake, the neutral compounds exhibit $\nu_{(\text{C}\equiv\text{N})} = 2224\text{ cm}^{-1}$ for TCNQCl_2 and 2218 cm^{-1} for TCNQBr_2 . The out-of-plane bending mode, $\delta_{(\text{C}-\text{H})}$, for TCNQ is also quite sensitive to the oxidation state of TCNQ. The $\delta_{(\text{C}-\text{H})}$ of 1 and 2 are 830 cm^{-1} and 866 cm^{-1} as compared to neutral TCNQCl_2 and TCNQBr_2 (848 cm^{-1} and 874 cm^{-1}) which reflect the reduced state of the molecules; the lithium salts of the reduced forms exhibit $\delta_{(\text{C}-\text{H})}$ modes of 828 cm^{-1} and 847 cm^{-1} respectively.³⁸

Thin films of 1 and 2 were prepared by spontaneous redox corrosion at the solid/solution interface by immersing sections of pre-cleaned silver foil into acetonitrile solutions of TCNQX_2

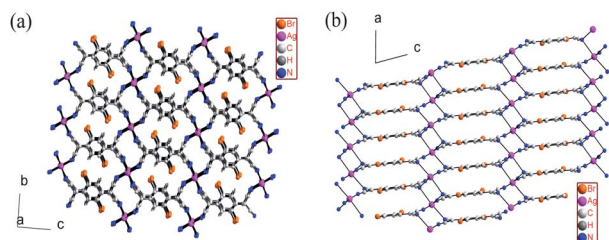


Fig. 2 Structure of $\text{Ag}(\text{TCNQBr}_2)$, (2): (a) viewed in the bc plane and (b) ac plane.

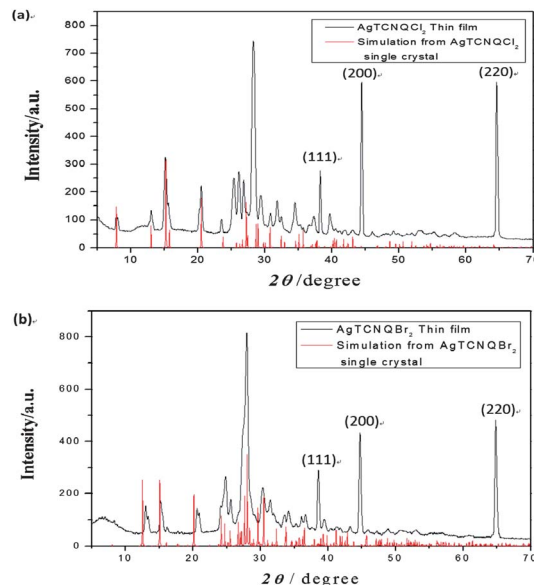


Fig. 3 A comparison of the powder diffraction pattern for a thin film and single crystal simulation of (a) AgTCNQCl_2 (1) and (b) AgTCNQBr_2 (2). The diffraction peaks of $\text{Ag}(\text{s})$ are marked in both figures.

for 30 minutes at room temperature. A comparison of the experimental powder X-ray diffraction pattern with simulations obtained from the single crystal structures confirms the presence of 1 and 2 in the films (Fig. 3). The SEM micrographs (Fig. 4) reveal micrometer-sized parallelepiped crystals that grow epitaxially along the propagation axis of TCNQ stacks much like the growth of nanoribbons and nanowires reported for $\text{Cu}(\text{TCNQ})$ phase I and $\text{Ag}(\text{TCNQ})$ which bodes well for preparing similar nanodevices of 1 and 2 by the same strategies.^{16–21,27–32}

Temperature-dependent conductivity measurements were performed on crystalline film samples of 1 and 2 using a two-probe method due to the small size of the crystallites. The data revealed that 1 exhibits good semiconducting behavior with a

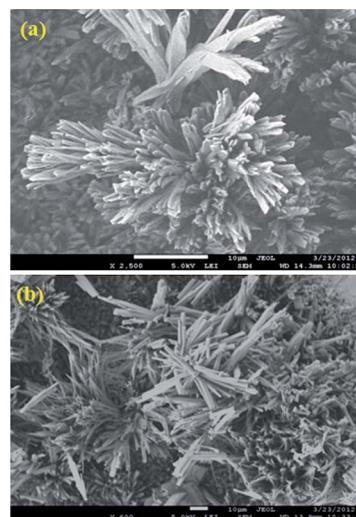


Fig. 4 SEM images for thin films of 1 (a) and 2 (b).

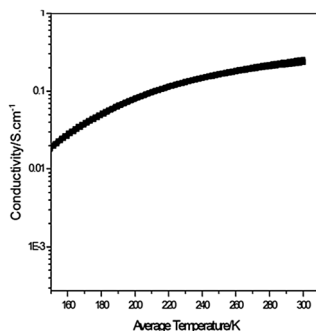


Fig. 5 Variable temperature conductivity measurement of **1**.

room temperature conductivity of 0.25 S cm^{-1} (Fig. 5) and an activation energy of 0.065 eV . In sharp contrast, compound **2** exhibits no recordable voltage signal with an applied current as low as 5 nA (the responding voltage is much higher than the limit of voltmeter), which is indicative of an insulator with a room temperature conductivity less than $1 \times 10^{-7} \text{ S cm}^{-1}$. These observations are consistent with the fact that there are regularly stacked TCNQ radicals in **1** but alternating short and long distances in **2**. The conductivity of **1** is essentially the same as that found for $\text{Cu}(\text{TCNQ})$ and is $\sim 10^3$ times higher than the originally reported $\text{Ag}(\text{TCNQ})$ material ($3.6 \times 10^{-4} \text{ S cm}^{-1}$).³⁴ The strong antiferromagnetic interactions between the dimerized radicals in compound **2** greatly reduces the electron mobility along the stack, resulting in insulating properties.

Evidence for switching behaviour was obtained by recording the non-linear I - V behaviour of crystalline films that were used for the typical conductivity measurements at room temperature. The strategy is to vary applied current in order to avoid the risk of melting or decomposing the sample with the corresponding responsive voltage being recorded. Given that **2** is insulating, only data for compound **1** were recorded. A negative differential resistance was observed at $\sim 50 \text{ V}$ after a current sweep in opposite directions ($0 \rightarrow 300 \mu\text{A} \rightarrow -300 \mu\text{A} \rightarrow 0$ for 2 times, Fig. 6a). A hysteresis loop was observed between 20 and 50 V . These results are in accord with a conducting state transition from a low resistance state to high resistance state, clear evidence of switching behaviour. The symmetrical shape of the I - V curve in the sweeping cycle indicates the full reversibility of this state transition. By plotting the resistance change with time, one can see that **1** exhibits as an intrinsic oscillation of resistance, which is suggestive of intrinsic thyristor behavior

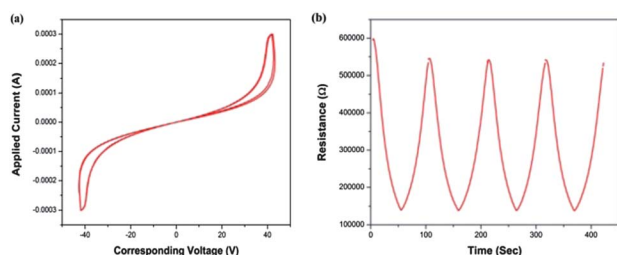


Fig. 6 Two direction sweeping non-linear conductivity measurements for **1**: (a) I - V plot (b) resistance vs. sweeping time plot.

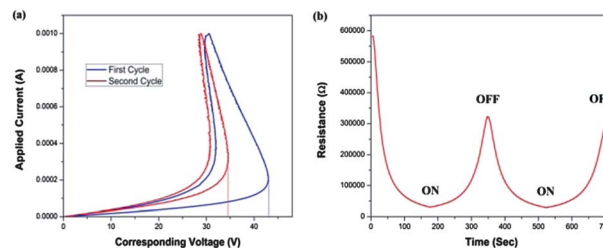


Fig. 7 One-direction sweeping non-linear conductivity measurement for **1**: (a) I - V curve and (b) resistance vs. sweep time plot for **1**. As a guide to the eye, lines were placed at the transition voltages ($\sim 44 \text{ V}$ for the first cycle and $\sim 35 \text{ V}$ for the second cycle).

(Fig. 6b). The current sweep in one direction was performed for two cycles (0 to $1000 \mu\text{A}$ to 0 , Fig. 7a) and it was found that the state transition appears at much lower voltages during the second cycle, specifically 35 V ($\sim 290 \text{ V cm}^{-1}$) as compared to 44 V ($\sim 365 \text{ V cm}^{-1}$) for the first one. The resistance *versus* time plot in Fig. 7b indicates a clear state transition between the on and off states. The shape of the curve appears to be reaching a plateau at the "ON" state, which indicates saturation of the state transition. The continuous feature of the curve indicates that the resistance of the second cycle starts at approximately half of the first cycle, which may be due to an uncompensated state transition under the high applied voltage without the erasing of the current from the opposite direction. This type of room temperature NDR behaviour has been reported for $\text{K}(\text{TCNQ})$ but at a much higher threshold voltage (100 V or 1920 V cm^{-1} at 300 K).³⁹ The mechanism of the non-linear behavior of $\text{K}(\text{TCNQ})$ has been postulated to originate from a current induced Peierls-to-non-Peierls state transition, as evidenced by the appearance of a dark stripe on the surface of crystal under a microscope that is observed to move across the crystal. Such a mechanism cannot be operative in the present case, however, because **1** contains homogenous stacks of TCNQ radicals and is not in a Peierls state.

In an effort to obtain insight into the mechanism of the observed switching behavior, we decided to measure the current-dependent electron paramagnetic resonance (EPR) spectra for **1** (Fig. 8a). A g -factor shift was observed with amplification of the applied current. Interestingly, the degree of g -factor shifting is proportional to the logarithmic value of the current (Fig. 8b). This response can be understood by considering a current promoted charge transfer from TCNQ radicals to

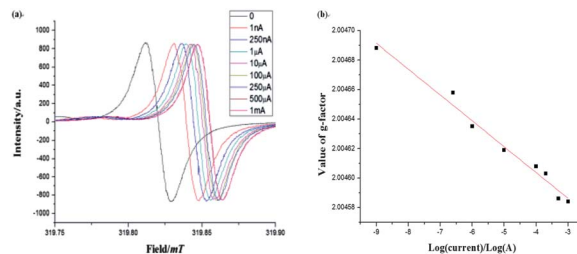


Fig. 8 EPR spectrum of **1** (a) under different current loading and (b) the linear fit of the g -factor values and the logarithm of the applied current. ((b), $R = 0.9770$).

the 5s orbital of Ag(I). In the initial state, the stacks of TCNQ radicals create a Mott insulating state and each frontier orbital of the TCNQ molecule is singly occupied by an electron; the 5s orbitals of Ag(I) are empty and lie at a higher energy than the SOMO (singly occupied molecular orbital) of the TCNQ radicals. Therefore, the effective gap of this semiconductor is a Hubbard-correlation-gap, which arises from on-site Coulomb repulsion.⁴⁰ Under the application of an applied current, the charge carrying electrons are promoted into the Ag 5s orbital as “hot electrons” which leads to partial charge transfer and a doping effect on the TCNQ stack. The doping effect decreases the average on-site Coulomb repulsion and consequently reduces the effective energy gap which leads to a more highly conducting state. Given that the energy scheme is very similar to a p–n junction, the diode *I*–*V* law can be adopted between the SOMO of TCNQ radicals and 5s orbitals of Ag cations (eqn (1)). The partial charge transfer will lead to the formation of uncoordinated TCNQ radicals in the stack, therefore it is expected that the *g*-factor shift arises from the doping of uncoordinated TCNQ radicals. This situation hints at a quantitative relationship between the applied current and the degree of charge transfer between the TCNQ radicals and Ag(I) cations.

$$I = I_s(\exp(\Delta V/V_T) - 1), \Delta V \propto \text{charge transfer degree} \quad (1)$$

These data and their implications are quite exciting as they are in excellent agreement with a mechanism that has been proposed on the basis of theoretical findings aimed at understanding the switching behavior of Cu(TCNQ) and Ag(TCNQ).^{22–26} The present findings constitute the first time that a quantitative mechanism has been elucidated for the non-linear *I*–*V* characteristic behaviour in a metal–organic hybrid material.

Conclusions

Electrocrystallization was used to prepare the new crystalline semiconductor Ag(TCNQCl₂) and the insulator Ag(TCNQBr₂). The presence of the chlorine substituents on the 2, 5 positions of TCNQ leads to a highly enhanced room temperature conductivity for Ag(TCNQCl₂) which is three orders of magnitude larger than the original Ag(TCNQ) material. Nevertheless, switching behaviour with a memory effect is observed at room temperature. Importantly, variable current EPR data have provided, for the first time, direct, real time evidence for the mechanism of switching as being due to the hybridization of Ag 5s orbitals into the conduction band. The ease of manipulation and fabrication of this material opens up the opportunity for the development of new generations of Ag(TCNQCl₂) nano-devices with useful potential applications for fast processing memory devices.

Notes and references

- 1 T. McGuire and R. Potter, *IEEE Trans. Magn.*, 1975, **11**, 1018.
- 2 C. S. Smith, *Phys. Rev.*, 1954, **94**, 42.

- 3 K. Y. Law, *Chem. Rev.*, 1993, **93**, 449.
- 4 D. W. Auckland, N. E. Brown and B. R. Varlow, *Electrical Insulation and Dielectric Phenomena*, IEEE, 1997, **1**, p. 186.
- 5 W. D. Brown and J. Brewer, in *Nonvolatile Semiconductor Memory Technology: A Comprehensive*, Wiley-IEEE press, Germany, 1997.
- 6 G. I. Meijer, *Science*, 2008, **319**, 1625.
- 7 M. H. R. Lankhorst, B. W. Ketelaars and R. A. M. Wolters, *Nat. Mater.*, 2005, **4**, 347.
- 8 G. Dearnaley, A. M. Stoneham and D. V. Morgan, *Rep. Prog. Phys.*, 1970, **33**, 1129.
- 9 H. Pagnia and N. Sotnik, *Phys. Status Solidi A*, 1988, **108**, 11.
- 10 M. A. Khan, U. S. Bhansali and H. N. Alshareef, *Adv. Mater.*, 2012, **24**, 2165.
- 11 A. S. Tayi, A. K. Shveyd, C. H. Sue, J. M. Szarko, B. S. Rolczynski, D. Cao, T. J. Kennedy, A. A. Sarjeant, C. L. Stern, W. F. Paxton, W. Wu, S. K. Dey, A. C. Fahrenbach, J. R. Guest, H. Mohseni, L. X. Chen, K. L. Wang, J. F. Stoddart and S. I. Stupp, *Nature*, 2012, **488**, 485.
- 12 D. Fu, H. Cai, Y. Liu, Q. Ye, W. Zhang, Y. Zhang, X. Chen, G. Giovannetti, M. Capone, J. Li and R. Xiong, *Science*, 2013, **339**, 425.
- 13 H. Ishiwara, M. Okuyama and Y. Arimoto, *Ferroelectric Random Access Memories: Fundamentals and Applications*, Springer-Verlag, 2004.
- 14 R. S. Potember, T. O. Poehler and D. O. Cowan, *Appl. Phys. Lett.*, 1979, **34**, 405.
- 15 R. S. Potember, T. O. Poehler and R. C. Benson, *Appl. Phys. Lett.*, 1982, **41**, 548.
- 16 A. K. Neufeld, I. Madsen, A. M. Bond and C. F. Hogan, *Chem. Mater.*, 2003, **15**, 3573.
- 17 D. Wang, J. G. Lu, X. Mo, C. Lou, Y. Yao and G. Chen, *Third conference on Nanotechnology*, IEEE-NANO, 2003.
- 18 C. Di, G. Yu, Y. Liu, Y. Guo, W. Wu, D. Wei and D. Zhu, *Phys. Chem. Chem. Phys.*, 2008, **10**, 2302.
- 19 K. Xiao, J. Tao, A. A. Puretzky, I. N. Ivanov, S. T. Retterer, S. J. Pennycook and D. B. Geohegan, *Adv. Funct. Mater.*, 2008, **18**, 3043.
- 20 X. Zhou, S. Wei and S. Zhang, *Langmuir*, 2008, **24**, 4464.
- 21 L. Ren, L. Fu, Y. W. Liu, S. Chen and Z. F. Liu, *Adv. Mater.*, 2009, **21**, 4742.
- 22 R. Müller, R. Naulaerts, J. Billen, J. Genoe and P. Heremans, *Appl. Phys. Lett.*, 2007, **90**, 063503.
- 23 E. I. Kamitsos, C. H. Tzinis and W. M. Risen Jr, *Solid State Commun.*, 1982, **42**, 561.
- 24 Z. Gu, H. Wu, Y. Wei and J. Liu, *J. Phys. Chem.*, 1993, **97**, 2543.
- 25 D. J. Flannigan, V. A. Lobastov and A. H. Zewail, *Angew. Chem., Int. Ed.*, 2007, **46**, 9206.
- 26 S. T. Park, D. J. Flannigan and A. H. Zewail, *J. Am. Chem. Soc.*, 2011, **133**, 1730.
- 27 J. J. Hoagland, X. D. Wang and K. W. Hipps, *Chem. Mater.*, 1993, **5**, 54.
- 28 S. Liu, Y. Liu, P. Wu and D. Zhu, *Chem. Mater.*, 1996, **8**, 2779.
- 29 N. Gu, W. Lu, S. Pang, C. Yuan and Y. Wei, *Thin Solid Films*, 1994, **243**, 468.

- 30 S. Liu, Y. Liu and D. Zhu, *Thin Solid Films*, 1996, **280**, 271.
- 31 S. Wakida and Y. Ujihira, *Jpn. J. Appl. Phys., Part 1*, 1988, **27**, 1314.
- 32 Z. Y. Hua and G. R. Chen, *Vacuum*, 1992, **43**, 1019.
- 33 R. A. Heintz, H. Zhao, X. Ouyang, G. Grandinetti, J. Cowen and K. R. Dunbar, *Inorg. Chem.*, 1999, **38**, 144.
- 34 L. Shields, *J. Chem. Soc., Faraday Trans. 2*, 1985, **81**, 1.
- 35 S. A. O'Kane, R. Clérac, H. Zhao, X. Ouyang, J. R. Galán-Mascarós, R. Heintz and K. R. Dunbar, *J. Solid State Chem.*, 2000, **152**, 159.
- 36 A. R. Harris, A. Nafady, A. P. O'Mullane and A. M. Bond, *Chem. Mater.*, 2007, **19**, 5499.
- 37 R. C. Wheland and E. L. Martin, *J. Org. Chem.*, 1975, **40**, 3101.
- 38 N. Lopez, H. Zhao, A. Ota, A. V. Prosvirin, E. W. Reinheimer and K. R. Dunbar, *Adv. Mater.*, 2010, **22**, 986.
- 39 R. Kumai, Y. Okimoto and Y. Tokura, *Science*, 1999, **284**, 1645.
- 40 Y. Lepine, A. Caille and V. Laroche, *Phys. Rev. B: Condens. Matter Mater. Phys.*, 1978, **18**, 3585.
- 41 H. Ikegami, C. Chong, H. Yamochi and G. Saito, *Mol. Cryst. Liq. Cryst.*, 2002, **382**, 21.
- 42 G. M. Sheldrick, *Acta Crystallogr., Sect. A: Found. Crystallogr.*, 2008, **64**, 112.